

Reno, Nevada
NOISE-CON 2007
2007 October 22-24

Airborne weaponry noise measurements [REVISED]

Micah Downing^a
Michael James^b
Bruce Ikelheimer^c
Blue Ridge Research and Consulting, LLC
13 ½ W. Walnut St.
Asheville, NC 28801

Christopher Hobbs^d
Wyle Laboratories, Inc.
241 18th Street South, Suite 701
Arlington, VA 22202

Sally Anne McInerny^e
Department of Mechanical Engineering
BEC 356D Business-Engineering Complex
University of Alabama at Birmingham
Birmingham, AL 35294-4461

ABSTRACT

Many aircraft noise models exist that estimate noise levels from military aircraft operations near airbases, along training routes, and within special use airspace, but these models do not include contributions to the noise by air gunnery and air fired missile operations. A new air-weaponry model is being developed to assess noise from these unique military operations. This paper describes the initial field measurements used to characterize air-weaponry noise sources and to evaluate propagation algorithms. Air gunnery noise data were collected from helicopter and fixed-wing aircraft operations. Missile launch noise data were collected from helicopter operations. For the air gunnery noise, important aspects of time-dependent waveforms and spectral descriptions for muzzle blasts and ballistic waves are discussed along with their directivity patterns. This analysis demonstrates that the positive impulse is the most stable metric for describing the muzzle blast. The peak is best for describing the ballistic wave; and the CSEL is best for the missile launch and thrust noise. For the propagation algorithm, the linear geometric theory of diffraction agrees well with the measured data. The development of an air weaponry model will be described in a companion paper.

1. INTRODUCTION

A number of aircraft noise models have been developed over the past 30 years to estimate noise levels from military aircraft operations near airbases, along training routes, and within special use airspaces. Predictions from these models are used to assess the potential impact (community and environmental) of current and proposed flight operations. The US Army has developed

^a Email address: Micah.Downing@BlueRdigeResearch.com

^b Email address: Michael.James@BlueRdigeResearch.com

^c Email address: Bruce.Ikelheimer@BlueRidgeResearch.com

^d Email address: Chris.Hobbs@wylelabs.com

^e Email address: SMcInerny@uab.edu

noise models for blast noise and supersonic shock waves generated by ground-based weapon systems. Current Department of Defense (DoD) noise models all use common aircraft and weapon system source noise databases, which are maintained by the Air Force Research Laboratory (AFRL), US Army Construction Engineering Research Laboratory (CERL), and Navy Facilities Engineering Command (NAVFAC). However, neither the models nor the databases include the noise contribution from air-gunnery or aircraft missile firing operations.

A new model is under development to calculate the air-borne weapon noise generated by air-weaponry operations. The goal of this project is to produce an air-gunnery noise model that will calculate both the single event noise, as well as cumulative noise, and provide acoustic visualizations for both planners and the public. The basis of the model's calculations will be positive impulse, peak pressures, and spectral content, so that the various acoustical metrics can be used to assess potential impacts.

The main objectives of this tool development project include the following:

1. To characterize the noise generated by airborne weapon systems. This will include important aspects of time-dependent waveforms and spectral descriptions of the noise sources, along with their dynamic directivity patterns. The data will be compiled so that it can be integrated into the noise databases used in various DoD models. A protocol for collecting airborne weapons systems acoustics data will also be developed.
2. To evaluate and refine current weapon noise propagation algorithms for application to airborne platforms. Refinements to topography and atmospheric propagation models will be made and the model will be enhanced to include the spectral time history.
3. Incorporate refined algorithms and additional input requirements into the new advanced aircraft noise simulation model being developed under SERDP Project SI-1304.¹ This will allow a means of visualizing the noise exposure of military aircraft operations as an aid to noise assessment and mitigation.
4. Transition the new computer model to DoD users, such as AFCEE and NAVFAC, enabling new technology to be quickly utilized in the assessment of environmental noise impacts.

This paper focuses on the first objective of characterizing airborne weaponry noise.

2. MEASURED DATA

A. Measured Data

Noise source characterization will be based on actual field measurements of airborne weaponry operations. The characterization of air-gunnery noise is complex due to the existence of multiple, sometimes simultaneous noise sources: muzzle blast, ballistic wave, propulsion noise (missiles), explosive projectile or warhead noise, and aircraft noise.

The combination of these sources also depends on the aircraft platform. For this project two field measurements were conducted. The first series of measurements involved firing of a 30 mm gun and, separately, training rockets from an AH-64 attack helicopter. Eighty-six gun firing runs and fifteen rocket firings were recorded for the AH-64 operations. The second series of measurements involved firing of the 30 mm gun from an A-10 fixed wing aircraft and a 20 mm

gun from the F-16, also a fixed-wing aircraft. Twelve A-10 and fifteen F-16 strafing runs were recorded during this second series of measurements. An array of 30 microphones provided basic angular coverage of the measured air gunnery noise for the AH-64D gun firing and missiles noise. For the F-16 and A-10 measurements, an array of 22 microphones was used. Most of the microphones were ground mounted with a few mounted on poles 13 meters above the ground. To capture the high frequencies in the sonic boom and muzzle blast, acoustic data were collected using microphones with a frequency response of 5 Hz to 40k Hz and a dynamic range of 46 to 164 dB. Data were recorded on a 24-bit data acquisition system at a rate of 96k samples per second.

A sample recording of an AH-64 gun firing event is shown in Figure 1. This event had the AH-64 helicopter firing its 30 mm canon in the forward firing position. For this run, 10 individual bullets were fired. In this figure, the top signal was recorded 365 meters forward of the firing point, the middle signal was recorded 90 meters forward of the firing point, and the bottom signal was recorded 60 meters behind the firing point. There is no sonic boom signature in the bottom signal, and, as expected, only the muzzle blast is seen. In the middle signal, the sonic boom and muzzle blast events overlap and have comparable peak overpressure values. At the furthest location (top), the sonic boom and initial muzzle blast are well separated, and the blast overpressures are significantly diminished.

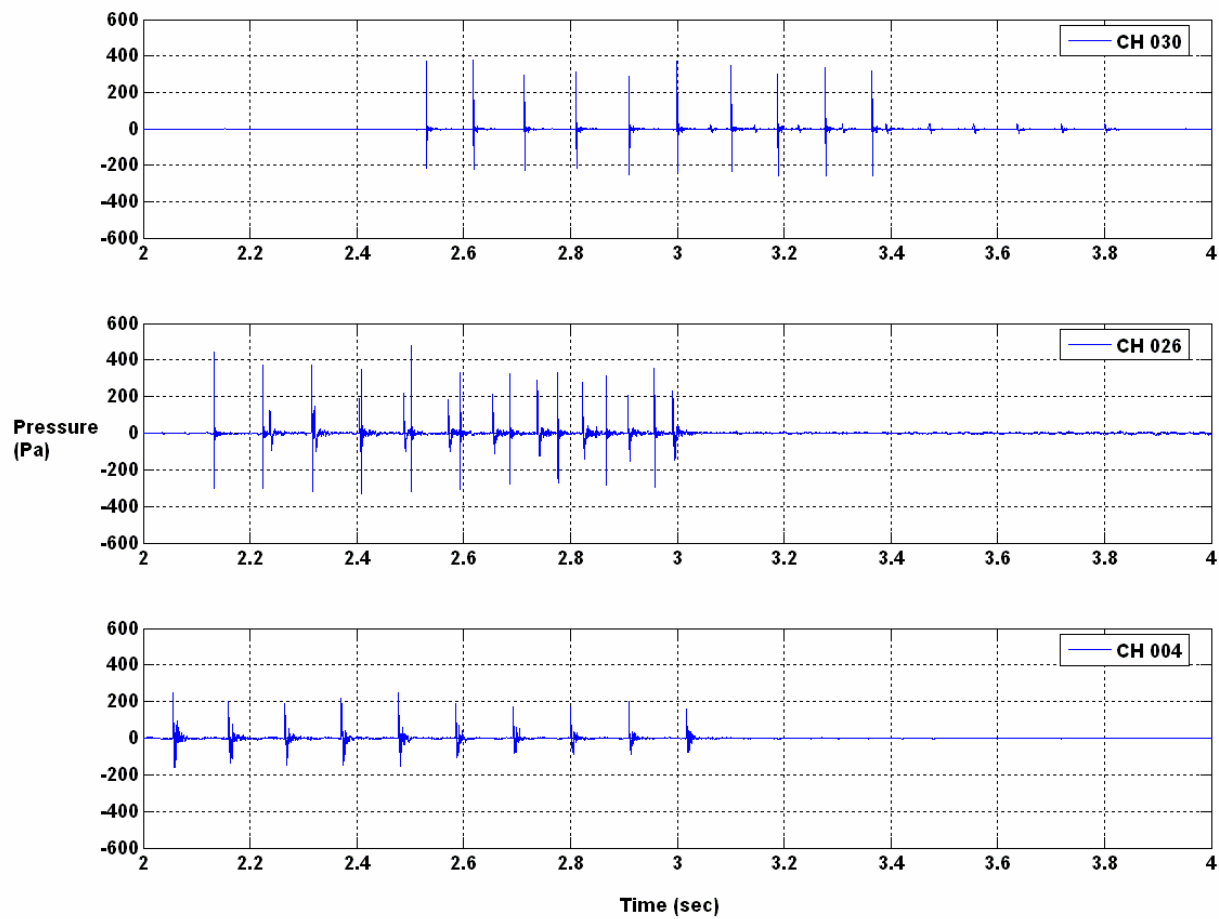


Figure 1: Sample pressure time histories for an AH-64 30 mm gun firing event.

Sample recordings of AH-64 rocket firings are shown in Figure 2; where the order of the plots is the same as in Figure 1. For the signal behind the firing point (bottom), the initial spike is the rocket ignition pulse. This is followed by the propulsion noise. In the middle plot, only the propulsion noise can be seen. In the top signal, the sonic boom is the first event occurring at 11.15s. The boom is followed by the propulsion noise and then the ignition pulse, which occurs at 11.30s. (Note that while the ignition overpressure travels at about the speed of sound, the missile and its propulsion system start out more slowly and pick up speed, reaching supersonic speed and overtaking the overpressure pulse before reaching the location of microphone 30.)

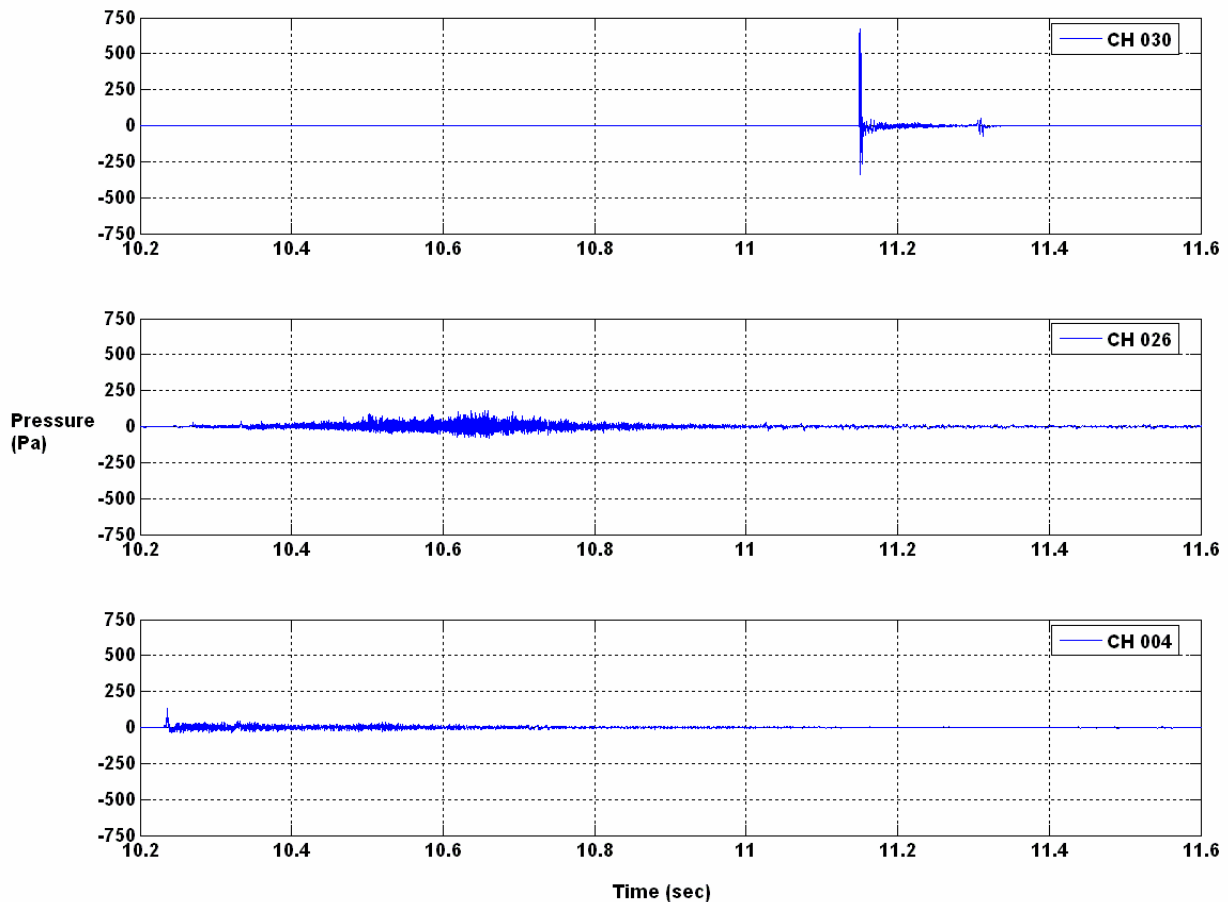


Figure 2: Sample pressure time histories for an AH-64 rocket firing event.

3. NOISE CHARACTERAZTION

A. Gunnery Muzzle Blast

For the analysis of the gun muzzle blasts, the time histories of all of the recorded data were analyzed to separate out the portions of the data where only the muzzle blast was recorded versus those where the sonic boom coincided with the muzzle blast. This separation results in the elimination of some muzzle blast data, but it is necessary because once the two signals are convolved it is impossible to evaluate them separately.

For this analysis each muzzle blast waveform was quantified using several different metrics. The metrics included: peak overpressure, sound exposure level, positive impulse, overall duration,

and positive pulse duration. Historically, peak overpressure has been used to quantify the magnitude of the muzzle blast. However, using peak overpressure produced a wide scatter in the data, obscuring any possible trends. A more stable metric was determined to be the positive impulse, which involves integrating the pressure over the duration of the positive pulse. The identification of the positive impulse is shown graphically in Figure 3.

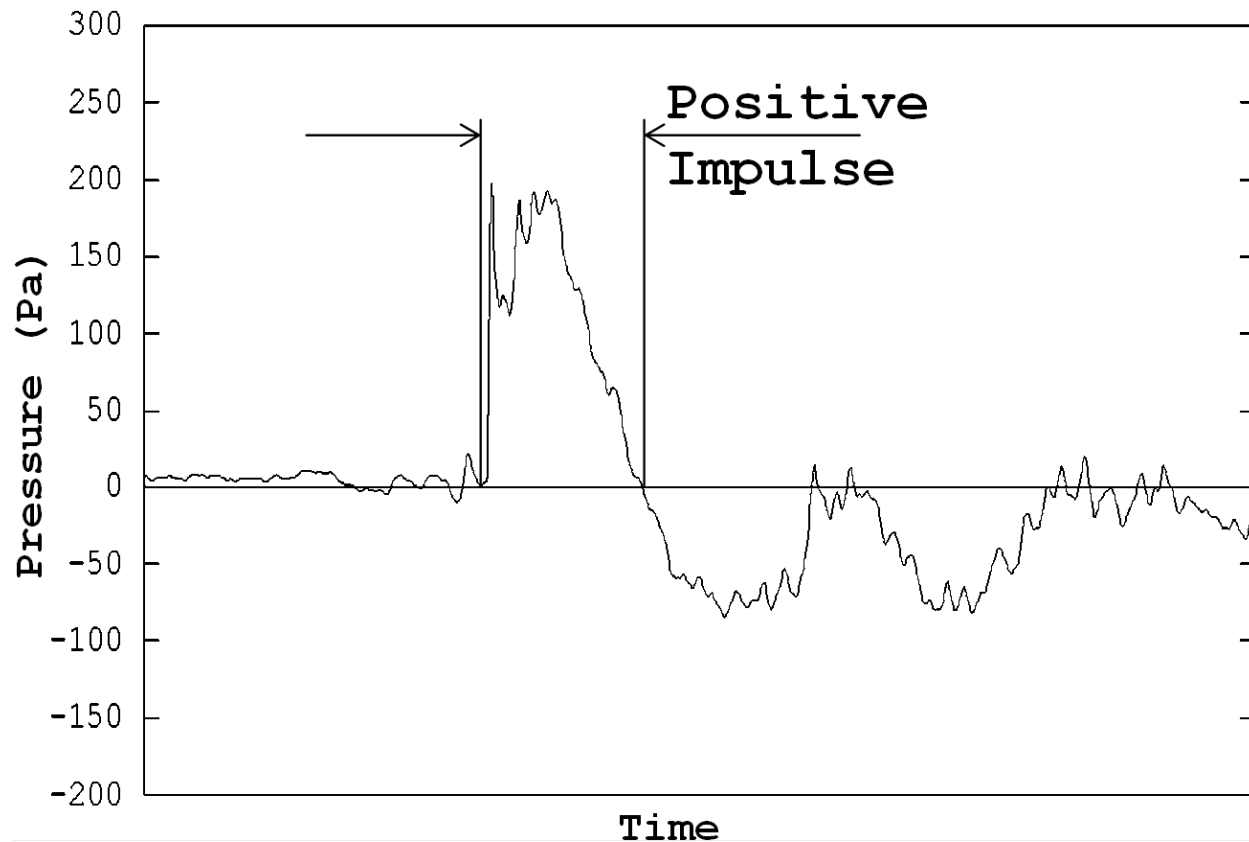


Figure 3: The identification of the positive impulse portion of a muzzle blast.

The positive impulse for each muzzle blast was calculated and used to determine the influence of directivity and aircraft operating state on muzzle blast noise levels. To isolate these trends, the acoustical data were normalized to eliminate known propagation effects. This normalization included the effects of spherical spreading, ground effects, and atmospheric attenuation. Once measurements were normalized for these propagation effects, general variations due to directivity and operating state can be evaluated. For this analysis the coordinate system used in traditional aircraft noise models^{2,3} is employed. Two angles are used to describe the directivity of the noise emissions. The angles are theta, θ , which describes the fore aft direction, and phi, ϕ , which describes the roll direction.

Once all of the muzzle blast data were normalized to one meter, the data were separated according to operating state (airspeed and firing altitude); but then no discernible differences could be observed between these groups. So, all of the data were analyzed together to determine one, composite directivity function. For each aircraft, the angular dependence is represented by a Fourier series approximation. For the AH-64 and A-10, the blast is symmetrical about the roll angle, ϕ , and is dependent on theta, θ . Thus, the Fourier series only has cosine terms. Estimates of the muzzle blast source positive impulse are obtained by combining the reference pressure

with the angular dependence. The approximations of the AH-64 and A-10 muzzle blast are given in equations 1 and 2, respectively:

$$PI(\theta) = 60.0dB + \left\{ \begin{aligned} &-0.895dB + 1.51dB \cos(\theta) - \\ &0.156dB \cos(2\theta) + 0.0144dB \cos(3\theta) - 0.0427dB \cos(4\theta) \end{aligned} \right\} \quad (1)$$

$$PI(\theta) = 65.5dB - \left\{ \begin{aligned} &-4.94dB + 5.80dB \cos(\theta) - 1.22dB \cos(2\theta) + \\ &0.566dB \cos(3\theta) - 0.348dB \cos(4\theta) \end{aligned} \right\}, \quad (2)$$

where $0^\circ < \theta \leq 180^\circ$. For the F-16, the blast is not symmetrical about the roll angle because of the placement of the gun port which is on the left side of the fuselage underneath the cockpit. Thus, the Fourier series approximation of the F-16 includes both cosine and sine terms, as well as a dependence on roll angle, ϕ . The resulting approximation can be expressed

$$PI(\theta, \phi) = 60.0dB + \left\{ \begin{aligned} &-4.69dB + 6.51dB \cos\left(\frac{\theta}{|\phi|}\right) - 1.62dB \cos\left(2\frac{\theta}{|\phi|}\right) + 0.197dB \cos\left(3\frac{\theta}{|\phi|}\right) - 0.337dB \cos\left(4\frac{\theta}{|\phi|}\right) - \\ &1.61dB \sin\left(\frac{\theta}{|\phi|}\right) + 0.291dB \sin\left(2\frac{\theta}{|\phi|}\right) - 0.444dB \sin\left(3\frac{\theta}{|\phi|}\right) + 0.185dB \sin\left(4\frac{\theta}{|\phi|}\right) \end{aligned} \right\}, \quad (3)$$

where $0^\circ < \theta \leq 180^\circ$. These directivity models were used to predict positive impulse levels at each of the measurement locations and these predictions then plotted against the actual measurements. See Figures 4-6. It can be seen that the Fourier series model provides an excellent fit.

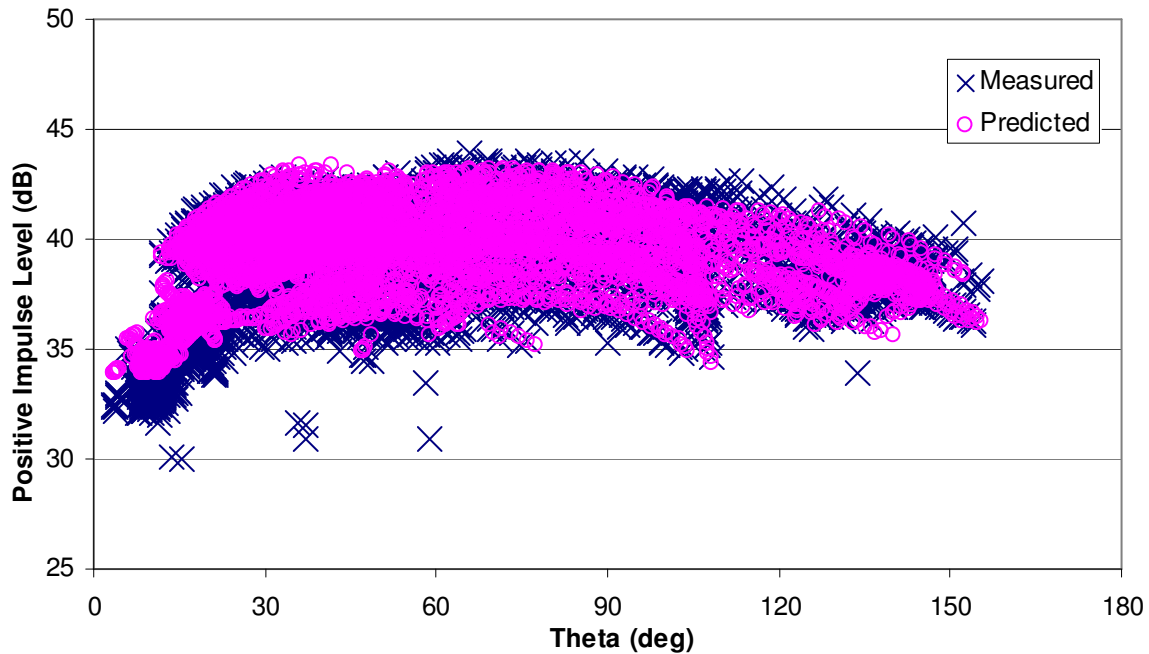


Figure 4: Predicted and measured AH-64 muzzle blast positive impulse plotted as a function of theta.

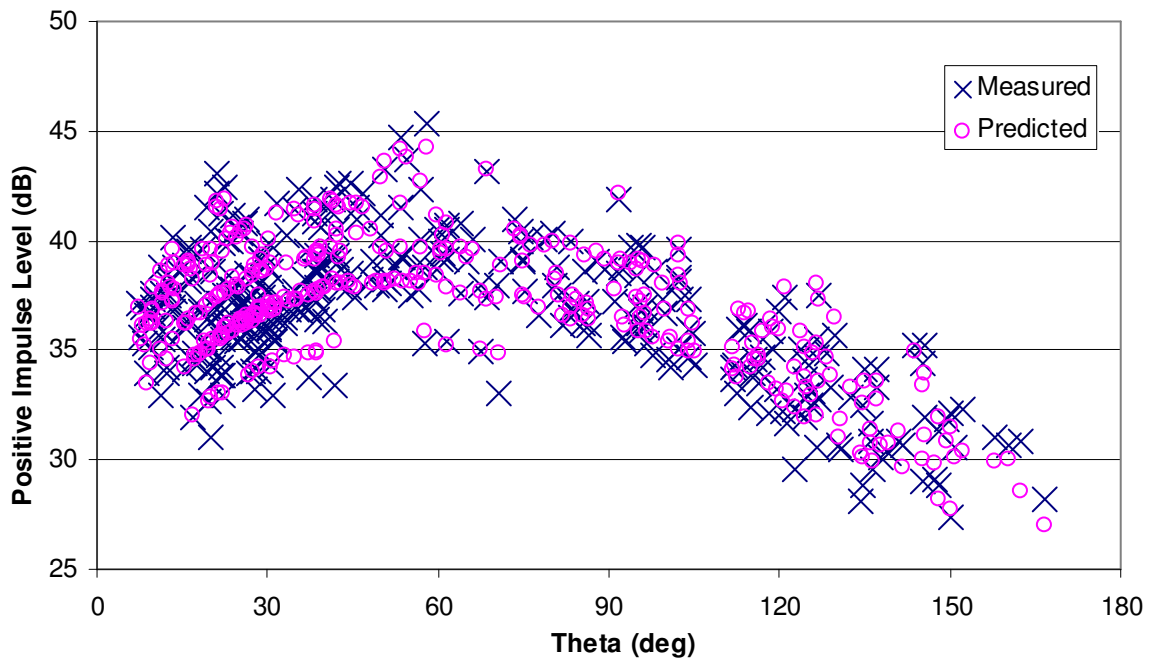


Figure 5: Predicted and measured A-10 muzzle blast positive impulse plotted as a function of theta.

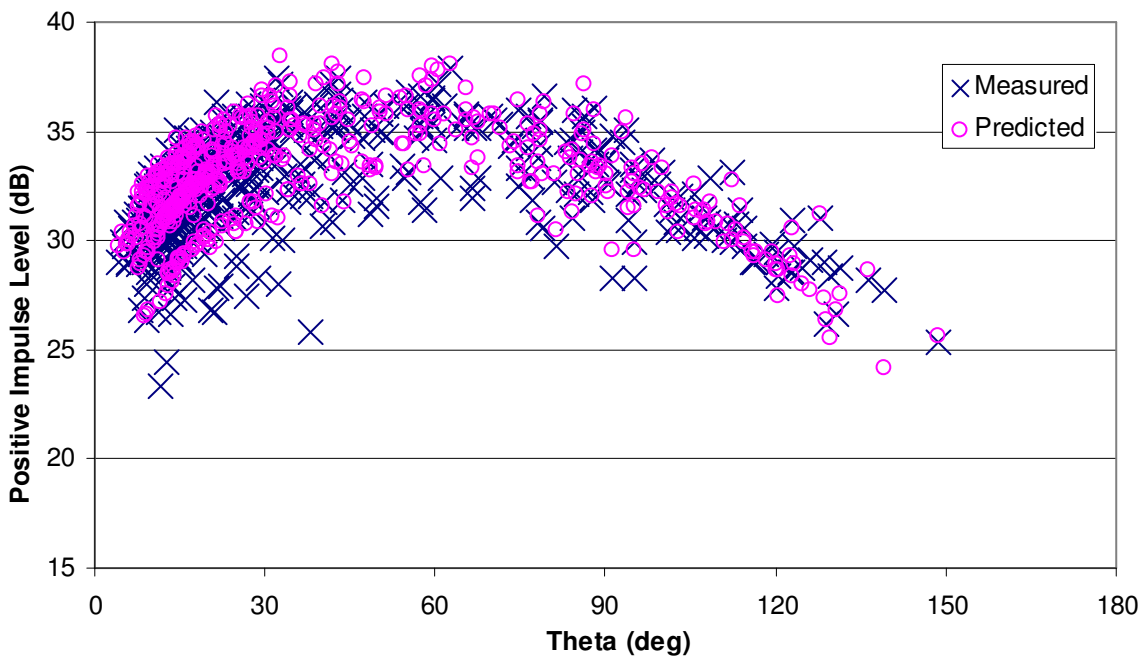


Figure 6: Predicted and measured F-16 muzzle blast positive impulse plotted as a function of theta.

Individual differences between predicted and measured impulse levels were examined in order to more precisely determine model accuracy. Five and ninety-five percentile bounds were defined, relative to the model estimate, as a function of theta for each aircraft/gun combination. These bounds denote values of positive impulse levels that equal or exceed 95% (or 5%) of the actual

measured levels. See Figures 7-9. These plots show that 90% of the measured values for all of the aircraft/gun noise sources are within ± 3 dB of the model estimates.

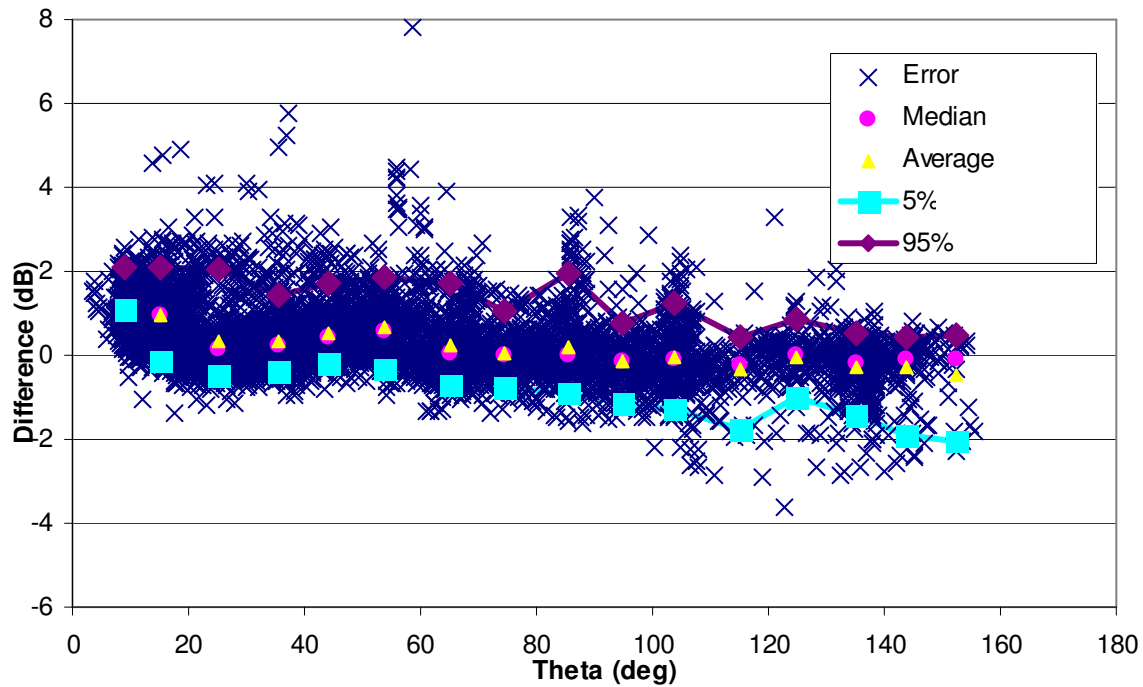


Figure 7. Differences between measured and predicted AH-64 muzzle blast impulse levels. Mean and median differences as well as 5% and 95% bounds are shown.

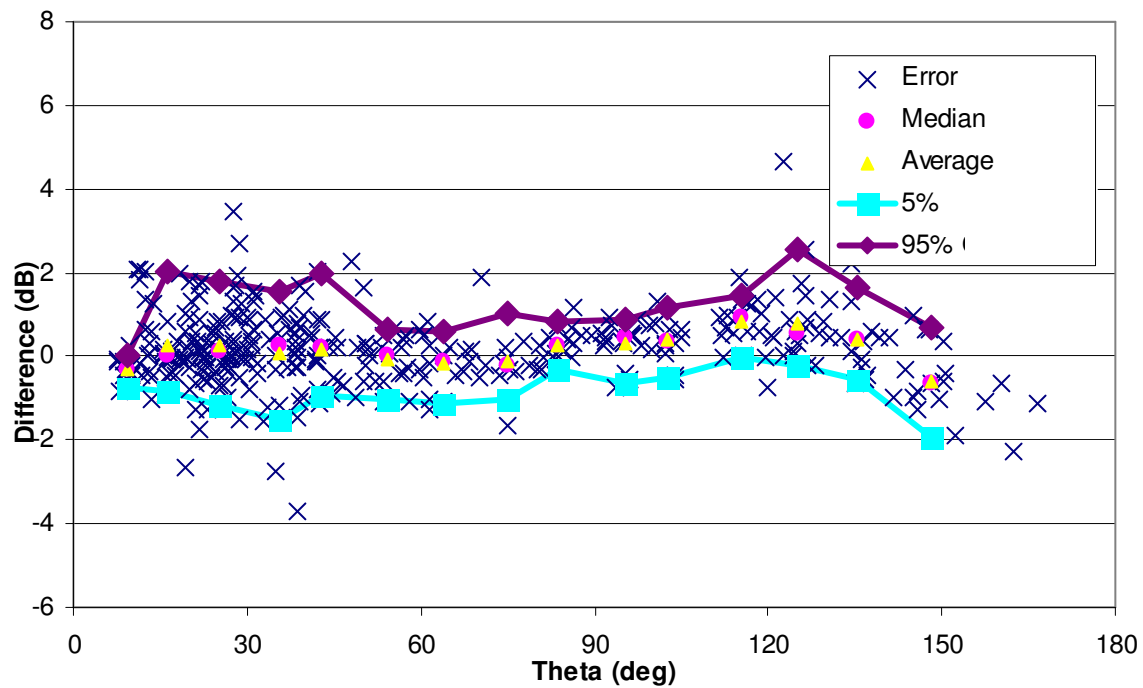


Figure 8. Differences between measured and predicted A-10 muzzle blast impulse levels. Mean and median differences as well as 5% and 95% bounds are shown.

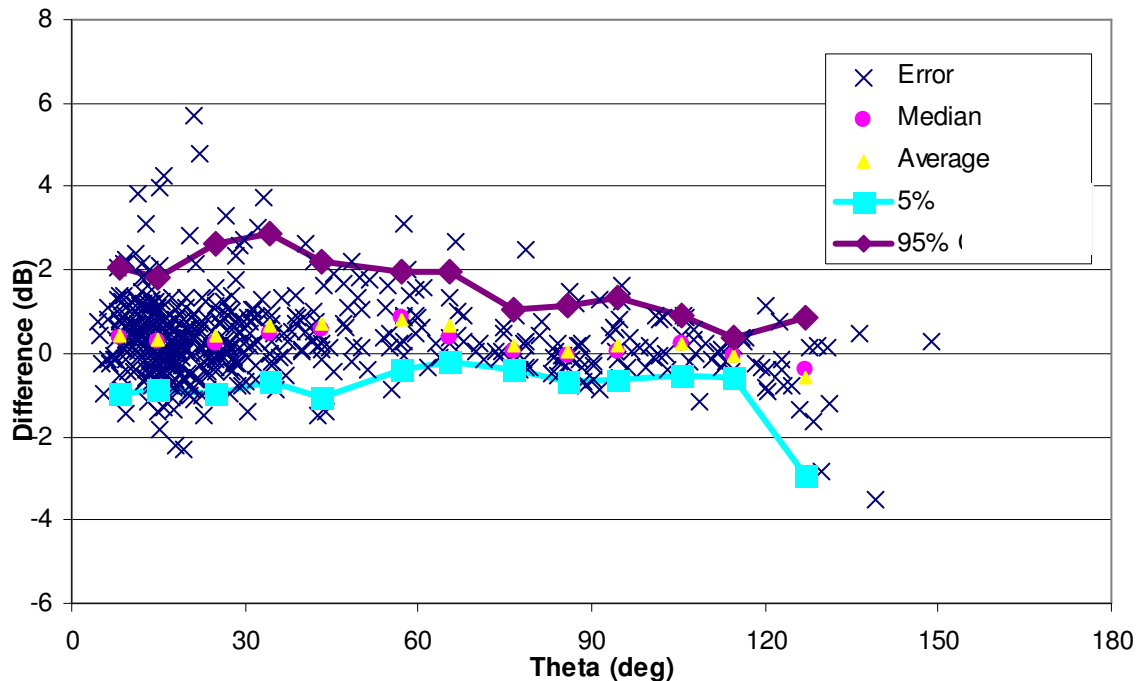


Figure 9. Differences between measured and predicted F-16 muzzle blast impulse levels. Mean and median differences as well as 5% and 95% bounds are shown.

B. Gunnery Sonic Boom

The bullets for all three aircraft/gunnery combinations travel at supersonic speeds, so that a sonic boom propagates to the ground forward of the firing point. The sonic boom from the projectile is referred to as the ballistic wave. For the AH-64, the ballistic wave of each of the bullets in a firing was identified. However, the rapid firing rate of the F-16 and A-10 guns resulted in greater overlapping of the individual muzzle blast waveforms, so the boom metrics were only calculated for the first and last ballistic waves in a firing. The metrics include peak overpressure, sound exposure level, positive impulse, and positive pulse duration. The measured data were compared to basic sonic boom theory.⁴ The comparisons demonstrate good agreement with simple theory. Figures 10 and 11 show the comparison between measured and theory of peak overpressure and duration, respectively for AH-64 gun firings. These comparisons demonstrate that simple sonic boom theory will work for air gunnery operations.

C. Missile Noise

Analysis and characterization of the various components of the helicopter launched missile noise (ignition overpressure, propulsion, sonic boom) is difficult, because: for locations relatively close to the launch, the ignition over-pressure pulse and the subsequent propulsion noise overlap, while for the measurement locations farther away and in the firing direction, the signal is dominated by the sonic boom. Only initial results are available for the helicopter launched missile noise. Measurements were made for static firings (helicopter in hover) and for firings in forward flight; but only static firing measurements and analysis results are presented here.

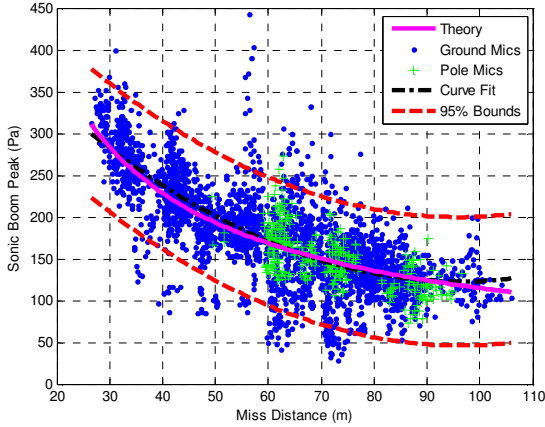


Figure 10. Forward fire, ballistic wave peak overpressure of AH-64.

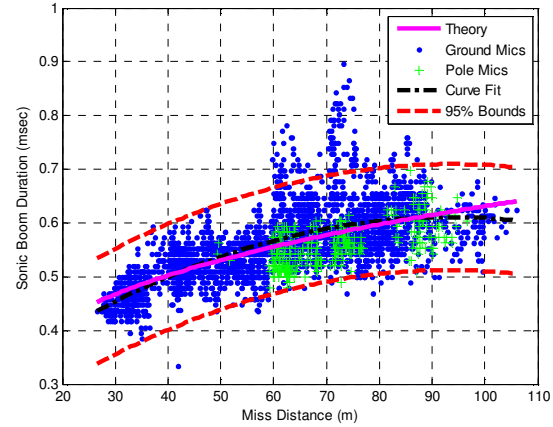


Figure 11. Forward fire, ballistic wave positive pulse duration of AH-64.

Figure 12 shows one of the boom signature recorded at the most distant measurement location. The first positive impulse is the boom from the leading edge of the missile. The rear missile shock (starting just after 11.151 s in the plot) is nearly lost in the positive impulse generated by the expanded plume. The rocket exhaust pressure is much greater than atmospheric, so that the plume expands rapidly downstream of the nozzle exit plane.

As a first cut at characterizing the noise at locations close to the firing location (i.e., those without sonic booms), un-weighted, C-weighted, and A-weighted “event” SELs were calculated. For the SEL calculations, the 10 dB down time period was determined from running rms levels (0.1 sec linear average, 90% overlap) for each recording. Figure 13 shows an example of rms levels and the 10 dB down time period. Once the SELs were calculated, they were normalized to 1 meter and examined for directivity effects. Figure 14 shows the theta dependence of the SELs, which reflect both ignition and propulsion noise. The source noise defined by CSEL is defined by the following equation:

$$CSEL(\theta) = 153dB + \{-0.0903dB - 1.18dB \cos(\theta) - 4.40dB \cos(2\theta) - 0.104dB \cos(3\theta) - 1.12dB \cos(4\theta)\}$$

for $0^\circ \leq \theta \leq 180^\circ$.

3. SUMMARY

An extensive database of air-weaponry noise data has been collected with the goal of creating a new environmental noise model. Four weapon systems were measured: the 30mm gun and Hydra 70 rocket on the AH-64 helicopter, the 30 mm gun on the A-10 and the 20 mm gun on F-16. A wide range of metrics were examined to determine which would be best suited for modeling. For gun fire, the positive impulse was selected as the most stable metric and useful for modeling. For each of aircraft gun combinations, a Fourier curve fit for directivity was created that accurately recreated the measured muzzle blast noise. The sonic boom from the gun fire was also examined. A simplified sonic boom model developed by Carlson was provided a good fit to the measured peak overpressures, as expected. Finally, the noise from rocket fire was examined in an initial step, and it was observed to have some complex features such as the ignition noise and sonic boom. In the initial analysis, ignition and propulsion noise were combined in an event SEL and a directivity pattern was developed. The sonic boom is composed

of two basic N-waves and will required modifications to Carlson's model for proper characterization of a rocket's sonic boom signatures.

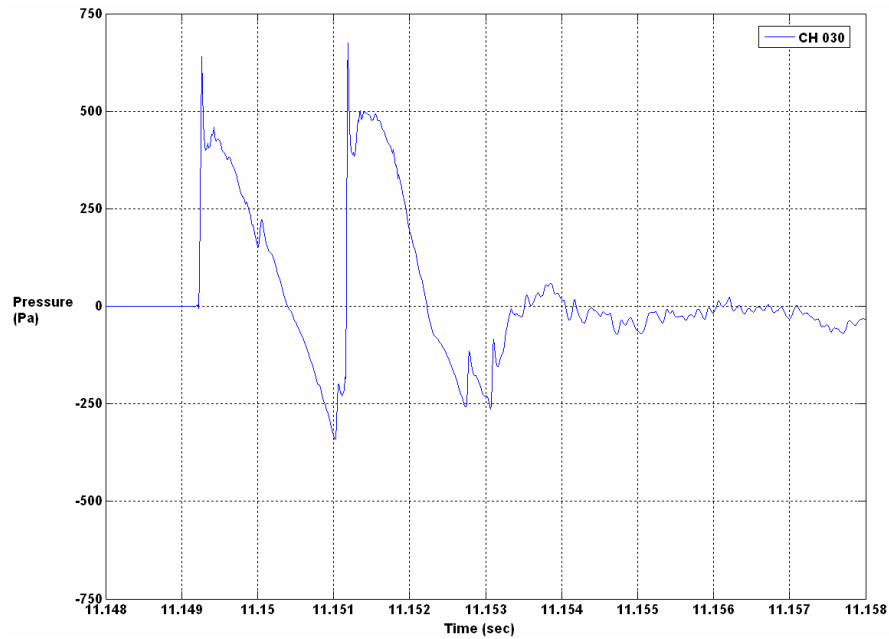


Figure 12. Sonic boom waveform for AH-64 training missile.

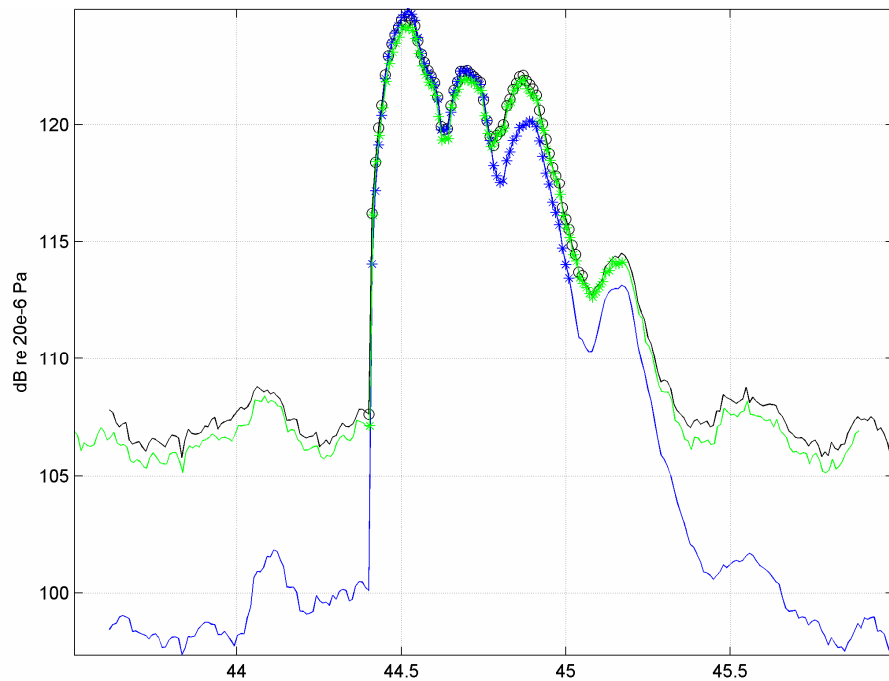


Figure 13. Rms (0.1s with 90% overlap) SPL for ignition and propulsion noise for an AH-64 missile firing. The black line is the un-weighted SPL, green is the C-weighted, blue is A-weighted. Symbols are used to show the 10 dB down time periods.

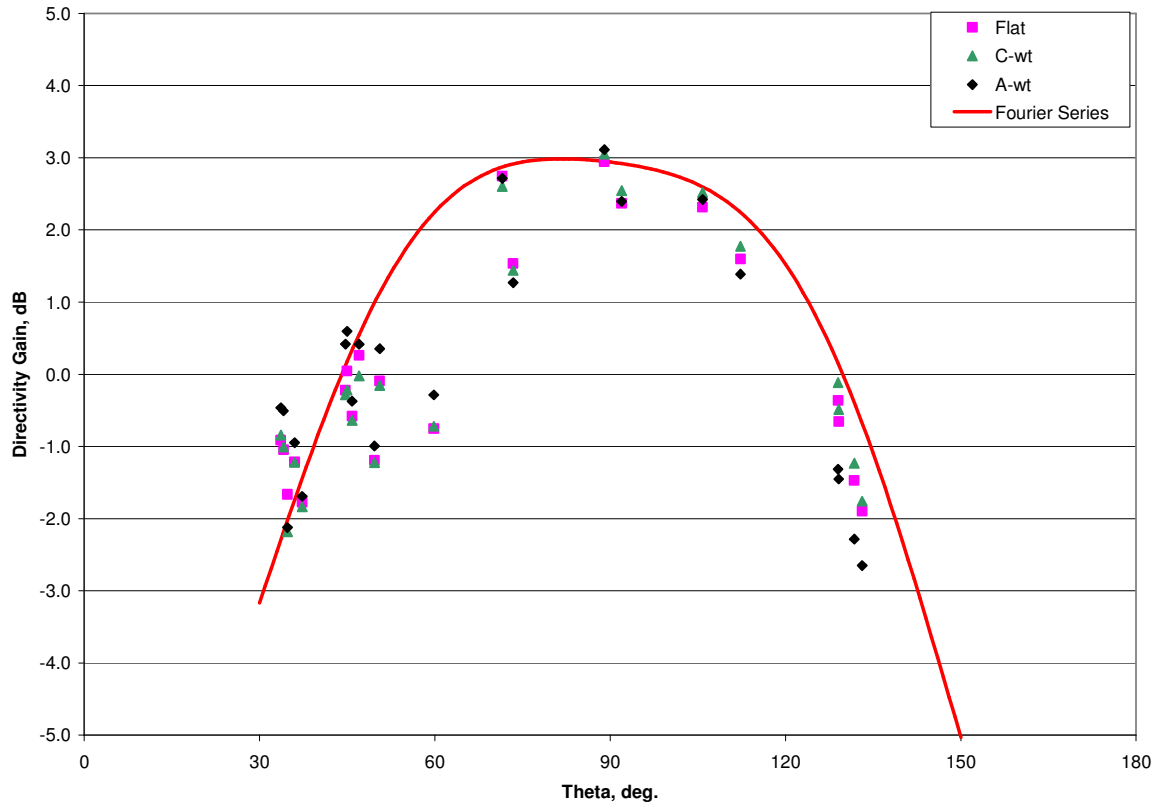


Figure 14. AH-64 missile ignition and propulsion noise directivity gain factor.

ACKNOWLEDGEMENTS

This research was supported wholly by the U.S. Department of Defense, through the Strategic Environmental Research and Development Program (SERDP).

REFERENCES

- ¹ K. J. Plotkin et al, "Advanced Acoustic Models for Military Aircraft Noise Propagation and Impact Assessment," SI-1304, Strategic Environmental Research and Development Program, 2002 to present.
- ² B. Ikelheimer and K.J. Plotkin, "Noise Simulation Model (NMSim) Users Manual," Wyle Report, WR 03-09, June 2005.
- ³ J. A. Page, K. J. Plotkin, J. M. Downing, and B. Ikelheimer, "Rotorcraft Noise Model (RNM 4.0) Technical Reference and User Manual," Wyle Report WR 04-11, April 2004.
- ⁴ H. W. Carlson, "Simplified Sonic-Boom Prediction," NASATP 1122, NASA Langley Research Center, Hampton, VA, 1978.